Gamma Spectra of Non-Enriched Thorium Sources using PIN Photodiode and PMT based Detectors

B.P. Jithin[1], Swapna Gora[1], V.V.V. Satyanarayana[2], O.S.K.S Sastri[1] and B.P Ajith[2]

[1]Central University of Himachal Pradesh, Bharat.
sastri.osks@gmail.com

[2]Inter University Accelerator Centre, New Delhi, Bharat.
ajith@iuac.res.in

Submitted on 14 December, 2012

Abstract

Gamma spectra of non-enriched Thorium Nitrate $ThNO_3$ salt is studied using an indigenously developed, low-cost portable gamma spectrometer, based on CsI scintillator mated to a PIN photodiode. The results of our study are compared with commercially available detectors based on NaI scintillators coupled to PMT detectors, that come with a certain cost and are bulky. Even though the intensity of various peaks are relatively less prominent in the spectrum obtained with the photodiode detector as compared to the PMT based one under same experimental conditions, longer duration for data collection and analysis using log plots were able to aid in reliable identification of all the dominant peaks in the source. The experiment gives good insights into nuclear radiation processes and various interactions that take place within the detectors. Finally, we repeated the experiment with a sample of Monazite from the sands of Kerala and confirmed the presence of Thorium deposits in it, thus proving the effectiveness of our portable gamma spectrometer for studying environmental radiation.

1 Introduction

In a previous paper [1], we have discussed the alpha spectrum of ^{212}Bi obtained from electrolysis of $ThNO_3$ salt, a non-enriched source available from chemical suppliers. The same salt can be used in powder form to obtain the gammas emmited by it. A low cost Gamma spectrometer has been developed by us [2] which uses a CsI scintillator mated to a PIN photodiode via an index matching optical grease interface. The design details are discussed in a separate pa-

per communicated recently. The electronics developed for our Alpha spectrometer [3] has been suitably modified, and the software CN-Spec has been upgraded to obtain the required spectral analysis along with added features for visualising surface plots for coincidence experiments [4]. The entire design has been prepared for commercial use by CSpark Research (India) [11] as GammaSpec1K. This work is in continuation with our efforts to developing Nuclear physics lab based on PER strategies for advanced UG experiments[6] using non-enriched sources and affordable equipment. In the presentation of this paper, we shall be focussing on studying gamma spectra of non-enriched Thorium samples. The first step before performing the experiment is to model the study, and this consists of arriving at the learning goals by enquiring into what we wish to accomplish. This is followed by understanding the theoretical considerations regarding the Thorium source, deduced from the experimental evidences documented in standard databases such as ENSDF[7]. Then, the physical system is modeled in terms of possible interactions of gamma radiation in the detection medium. All this has been elaborated in the second section. In the third section, we focus on the experimental design strategy and model the measurement apparatus elucidating the principle of operation, the capabilities of the detection units and data acquisition. This is followed by the analysis of spectra and discussion of various aspects that characterize them in section 4. Finally, we extend our study to validate the presence of Thorium deposits in Monazite found in the sands of Kerala and draws conclusions.

2 Modeling

In model construction, as a first step, we need to answer the following simple questions?

1. Which real world phenomenon do we wish to study?
   Ans: We wish to study the gamma radiation emitted by Monazite sand commonly found in beaches of the Indian peninsula. It is known from literature, that the radioactive deposits in the sands contain deposits of Thorium and trace amounts of Uranium. We have with us in our laboratory, a non-enriched source of Thorium in the form of $ThNO_3$ salt, so it will be appropriate to first conduct the experiment on this source, and later apply the obtained knowledge to understand the radiation emitted by the Monazite sand.

2. Which aspects of the real-world system are included in the model?
   Ans: One of the naturally occurring radioactive series is that of Thorium, whose data is well documented in ENSDF. It goes through a series of alpha and beta decays during which the daughter nucleus might be in one of its excited states that undergoes gamma

decays. We focus only on obtaining the energies of these gamma emissions in our model.

3. What is being ignored?
   Ans: We are ignoring the detection of alpha and beta. Also, we are not interested in the intensities of the gamma emission that are quoted to be less than 10%, and also energies which are below 100 keV, keeping in mind the capabilities of our gamma spectrometer.

4. What principles are needed to describe the phenomenon?
   Ans: The interaction processes that gamma undergoes during the deposition of its energy within the detector medium needs to understood. That is, the principles of compton effect, pair production and photo-peak are to be described while analyzing the obtained spectra.

5. What parameters are needed in the model?
   Ans: If the experiment is being introduced at the UG level, we could just focus on determining the Q values for alpha and beta for the various daughter nuclei of Thorium and try to make them appreciate the theoretical reasoning behind the observed series. At PG level, one could also include the total angular momentum I and parity pi values in the data and emphasize on the selection rules that are resulting in the various decays being observed.

6. What approximations or idealizations are made ?
   The approximations result from the limitations that are imposed due to the capabilities of the detector. For example, the FWHM of the spectrometer naturally dictates the resolution of the gammas that can be observed.

Further, since the gamma spectrum that is being studied is that of Thorium and we have already utilised a non-enriched source of ThNO3 salt for studying alpha spectra[1], we have extended the experiment to also include the study of spectra obtained from this salt using both the gamma spectrometer that we have developed[2] and the existing one in the lab based on NaI coupled to PMT. This would help in comparative analysis. Based on all of the above considerations, we have designed the lab specific learning goals as:

1. understanding the nuclear radiation processes that are resulting in the gamma emissions of Th,

2. comprehension of the various interactions that are responsible for energy deposition in the detectors

3. a broad overview of the measurement processes, and comparative analysis of spectra obtained from two different types of detection techniques.

4. application to studying samples that contribute to environmental radiation

2.1 Modeling the Source

The source is a non-enriched radioactive sample composed of thorium nitrate ($Th(NO_3).5H_2O$) in powder form which has ^{232}Th and its various daughter products in secular equilibrium via decays associated with alpha and beta emission. De-excitation of daughter products from these decays are accompanied by emissions of gamma rays. Alternatively, we have also used a sample of Monazite sand obtained from the beaches of kerala that contains Thorium deposits and some trace amounts of Uranium as well. Our focus is on:

1. Identifying the various gammas present in the two samples.

2. Appreciate the potential of the non-enriched, naturally radioactive Monazite sand as a safer alternative.

3. Comparing the performances of CsI mated to PIN photodiode to that of NaI scintillator attached with a Photo Multiplier Tube(PMT).

The learners' goals are to (i) model the gamma decays theoretically and (ii) obtain the quantitative predictions of observable phenomenon, in this case, the gamma energies that are emitted by Thorium samples.
The first objective is achieved by making the students observe the level diagrams of ^{232}Th and its entire decay chain from ENSDF website. The alpha and beta decays that the various nuclei undergo are governed by the respective selection rules. The intensities to the ground and excited states are given along with the respective HF in case of alpha and log ft values in case of beta decays. Whenever a given parent nucleus decays into one of the excited states of the daughter, it is followed by gamma emission so as to reach the ground state. All these adopted gamma decays from various experiments performed by different groups across the world are given in the level structure diagrams of the nuclei and the students are asked to choose the levels resulting in gammas which are having intensity greater than 10% for the purpose of study. The resultant flow diagram is shown in Fig 1.

2.2 Modeling of Physical System

Gamma rays have high penetrating ability as compared to alpha and beta particles, and it is not possible to directly measure their energy with a semiconductor based detector such as a photodiode. Therefore, typically a scintillation crystal is used, which absorbs the gamma ray energy and emits a proportional number of scintillation photons whose wavelengths lie in the visible region. The difference in absorption probabilities for a semiconductor and scintillation detector is very evident in the log plot in Figure 2, and one can see that a simple silicon detector has a next to nothing chance of absorbing gamma rays with energies beyond 200keV.

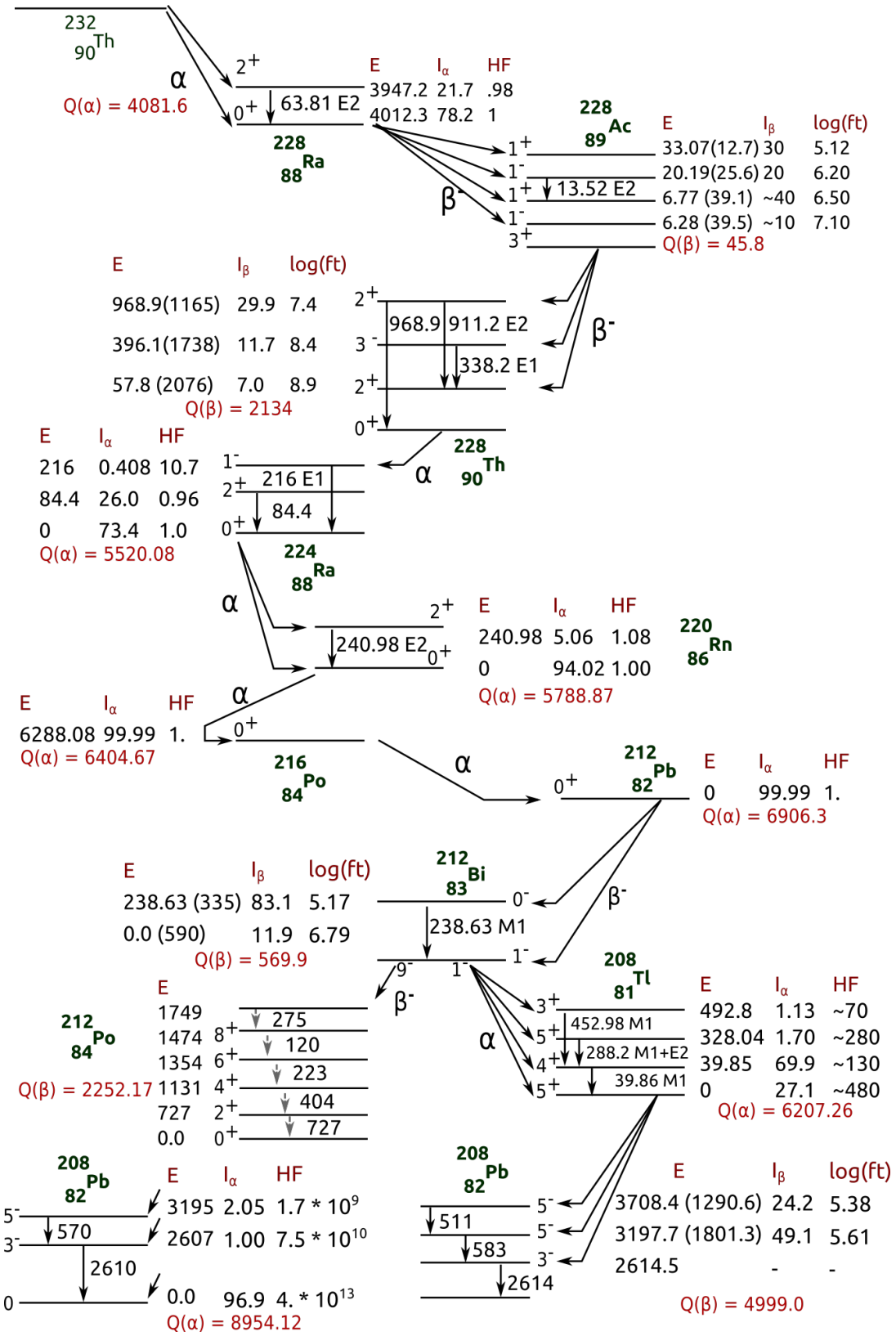

Figure 1: The decay chain of ^{232}Th highlighting the level structures of daughters that result in $>$ 10% gamma intensities.

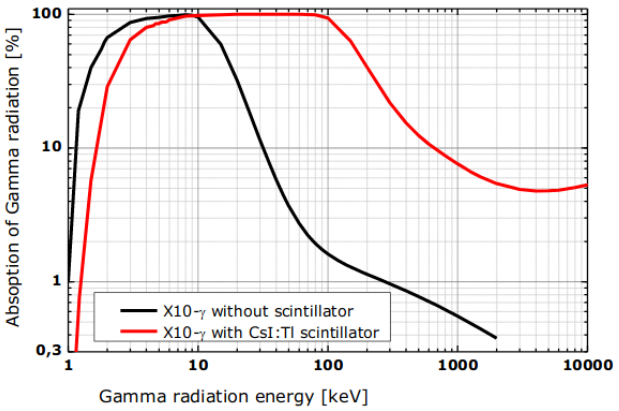

Figure 2: Absorption probability of gamma rays in a solid state detector as a function of their energy with and without scintillator attached. Source:[13]

2.2.1 Interaction Processes:

Since the gammas do not attenuate appreciably in air, we need to consider only the interactions that take place within the detector. The following competing processes define the interaction of photons with matter, or in our case, gamma rays with the scintillation crystal:

Photoelectric effect: The incident gamma ray transfers its entire energy to an electron in the scintillator which then travels along the scintillator material creating a number of scintillation photons proportional to its initial energy.

Compton scattering: This occurs when the incident gamma ray interacts with a free electron and loses some energy in the recoil process. The energy loss is characterized by a loss in frequency of the incident gamma ray since its velocity must be constant. The resultant scintillation photons produced by the recoil is also lower than that of the photoelectric process since the scattered gamma ray still contains a part of its initial energy.

Pair production: For gamma rays with energies(E) greater than 1.022MeV which corresponds to twice the rest mass energy of an electron, an electron-positron pair may be created in accordance with Einstein's mass-energy relation. The energy excess is transferred to the pair. The positron annihilates with the production of a pair of 511keV gamma rays. The net energy deposited can be one of the following

- Initial Energy of the gamma ray(E). This implies that both 511 keV photons deposited their energy in the scintillator, and the excess energy also created a proportional number of scintillation photons.
- One of the photons escaped the material, resulting in the total deposited energy being only $E - 511keV$. This position in the spectrum is called a single escape peak.
- Both the annihilation photons escaped the material, resulting in $E - 2 * 511keV$ being deposited. This creates what is known as a double escape peak.

2.3 Modeling Outcomes

The students at UG level can easily determine the Q_α and Q_β values of the nuclei using Binding energy values obtained from Semi-Empirical Mass Formula based on the Liquid Drop Model. This provides the theoretical basis as to why the sequence, of αs and βs in Thorium series, is the way it is. $Q_\beta \leq 0$ and $Q_\alpha >> 0$ implies, the nucleus is β stable and the only mode of decay is through α. Whenever, $Q_\beta > 0$, it is the more preferred mode of decay.

At the PG level, the students can be guided to observe that most of the β decays are proceeding through parity changing forbidden transitions to the excited states of the daughter nuclei. Further, it is seen that for the transitions to proceed to the ground state of the daughter, we have $\Delta I \geq 2$. An analysis of the log ft values of β-decays in the A 221 Actinide region has revealed that the first forbidden transitions have comparable values to that of the allowed transitions[12]. The various gammas from the level sequence diagrams in Fig.1 are compiled in Table 1. Even though all these energies are expected to be seen, the limitations and interactions of the detection unit places certain restrictions, which will be discussed later.

3 Experimental Design

There are different ways to design an experiment so as to validate the correctness of the results. One such design strategy that is incorporated here, is to obtain the data through two different techniques and perform a comparative analysis. Franklin [17] discusses this as the first epistomological strategy which is effective in arriving at valid results:

> A hypothesis receives more confirmation from different experiments, where different measurement instruments are used, than from the repetition of the same experiment,where the same apparatus is used each time. This reference to different experiments is due to the fact that the theories that underlie the various apparatus are different; Since the results of an experiment are strongly related to the theories underlying the different apparatus employed, one may regard the results of performing an experiment using different measurement instruments as being obtained from different experiments.

The gammas emitted by the $ThNO_3$ powder are studied using two different detection units. One is the commercially available NaI(Tl) scintillator coupled to a PMT and the other is our own indigenously developed detection unit consisting of CsI(Tl) scintillator mated to a PIN photodiode using an index matching glue. Here, the methods for depositing the energy of the scintillation photons, generated from gammas incident on the NaI(Tl) or CsI(Tl) detectors, are different and hence the measurement instruments differ in their principle of operation

Parent	Process	Daughter	I_p^π	$I_{d*}^\pi \rightarrow I_d^\pi$	I_α / I_β	HF/ logft	E_γ (keV)
$^{232}_{90}Th$	α	$^{228}_{88}Ra$	0^+	$2^+ \rightarrow 0^+$	21.7	0.9	63.8
$^{228}_{88}Ra$	β	$^{228}_{89}Ac$	0^+	$1^- \rightarrow 1^+$	20	6.2	13.5
$^{228}_{89}Ac$	β	$^{228}_{90}Th$	3^+	$2^+ \rightarrow 0^+$	29.9	7.4	968.9
				$2^+ \rightarrow 2^+$			911.2
				$3^- \rightarrow 2^+$	11.6	8.4	338.2
$^{228}_{90}Th$	α	$^{224}_{88}Ra$	0^+	$1^- \rightarrow 0^+$	0.4	10.7	215.9
				$2^+ \rightarrow 0^+$	26.0	0.9	84.4
$^{224}_{88}Ra$	α	$^{220}_{86}Rn$	0^+	$2^+ \rightarrow 0^+$	5.1	1.1	240.9
$^{212}_{82}Pb$	β	$^{212}_{83}Bi$	0^+	$0^- \rightarrow 1^-$	83.1	5.2	238.6
$^{212}_{83}Bi$	α	$^{208}_{81}Tl$	1^-	$3^+ \rightarrow 4^+$	1.1	70	452.9
				$5^+ \rightarrow 4^+$	1.7	280	288.2
				$4^+ \rightarrow 5^+$	69.9	130	39.8
$^{212}_{84}Po$	α	$^{208}_{82}Pb$	18^+	$5^- \rightarrow 3^-$	2.1	$1.7 * 10^9$	570
				$3^- \rightarrow 0^+$	1.0	$7.5 * 10^{10}$	2610
$^{208}_{81}Tl$	β	$^{208}_{82}Pb$	5+	$5^- \rightarrow 5^-$	24.2	5.4	510.8
				$5^- \rightarrow 3^-$			583.2
				$3^- \rightarrow 0^+$	49.1	5.6	2614.5

Table 1: The I^π values for the parent and those of the excited states of the daughter and that of the final state to which the transition takes place are indicated.

in producing the final output voltage corresponding to the same gamma energies.

3.0.1 Principle of operation:

In case of the photomultiplier tube(PMT), the scintillation photons eject a proportional number of electrons from the photocathode of the PMT, which then accelerate towards an adjacent dynode which is maintained at a higher potential. The electrons thus ejected are higher in number due to the energy gained whilst accelerating through the potential, and are now directed towards a second dynode which is maintained at an even higher potential. This sequence of events through multiple dynodes results in an amplification of the initial incident photopulse, and a proportional voltage spike is created at the output of the PMT.

On the other hand, the semiconductor photodiode's PN junction is connected in reverse bias mode so as to create a depletion region that acts as an ionization medium to convert their energy into electron-hole pairs which move towards the electrodes due to the applied electric field. The charge thus generated is proportional to the energy of the incident gamma ray.

The length of the scintillator decides the photopeak efficiency. In other words, a longer scintillator tube results in more gamma rays depositing their entire energy in the crystal, and contribute to the photopeak rather than the Compton edge. The size of our CsI(Tl) detector is $10mm \times 10mm$ with a thickness of $8mm$ as compared to the NaI(Tl) detector available in the lab that has approximately 5 times larger dimensions.

3.1 Modeling the Measurement Apparatus:

The PMT from **Ortec** includes a preamplifier, and its output was input to a shaping amplifier stage by **CAEN(N968)**[15]. The shaper output of 3uS rise time was processed using a **4K USB Multi Channel Analyzer** developed by us[16], and the spectrum was acquired using our **CNSpec** Software. The PMT needs a bias voltage, which is typically in the range of 550 to 1100 V. A bias voltage of 730Volts was maintained for the PMT used here, so as to obtain the 1332 keV peak from ^{60}Co to be somewhat nearer to the half way mark in the 4K channels. For calibration, spectrum from ^{60}Co was taken, and the 1332keV peak was located at channel 1824.86. Then a second spectrum was acquired from ^{137}Cs, and the 662keV peak was located at channel 931.79. These two datapoints were used to create a straight line calibration polynomial. Since these two chosen peaks are far apart, errors in slope calculation arising due to small variations in the gaussian fitting based centroid estimation are minimized.

'GammaSpec-1K' gamma spectrometer setup, that can measure gamma energies upto 3 MeV developed by us (is shown in Figure 3). The various stages of signal processing electronics are shown as an inset. The compact detector unit, consisting of the CsI scintillator mated to PIN photodiode and the associated electronics, is the just the size of a smart phone (with about 4 times the thickness). It is powered by the USB of a laptop. Data from the 1K MCA is acquired via same USB cable and the spectrum builds dynamically in our software 'CNSpec' written in the Python language with FOSS tools[4]. Gaussian curve fitting, log plots, sum of events and other analysis and report requirements are incorporated into the software.

The source is to be placed in front of the 8mm hole behind which the detector is housed. The detector's peak sensitivity is around 540nm[13] and hence it is covered by an Aluminium foil of 20 microns thick, so as to block any stray visible spectrum light which was not generated by the scintillator.

The instrument is factory calibrated using ^{60}Co which has two sharp peaks at 1173 keV and 1332 keV. For this unit, the centroid channel for the 1.33MeV peak was calculated using gaussian fitting to be 503, and the corresponding calibration polynomial is $y = \frac{1332}{503} * x$. The FWHM of this peak is found to be 80 KeV. It is observed that at the lower end of the spectrum, spurious events are getting recorded due to the noise

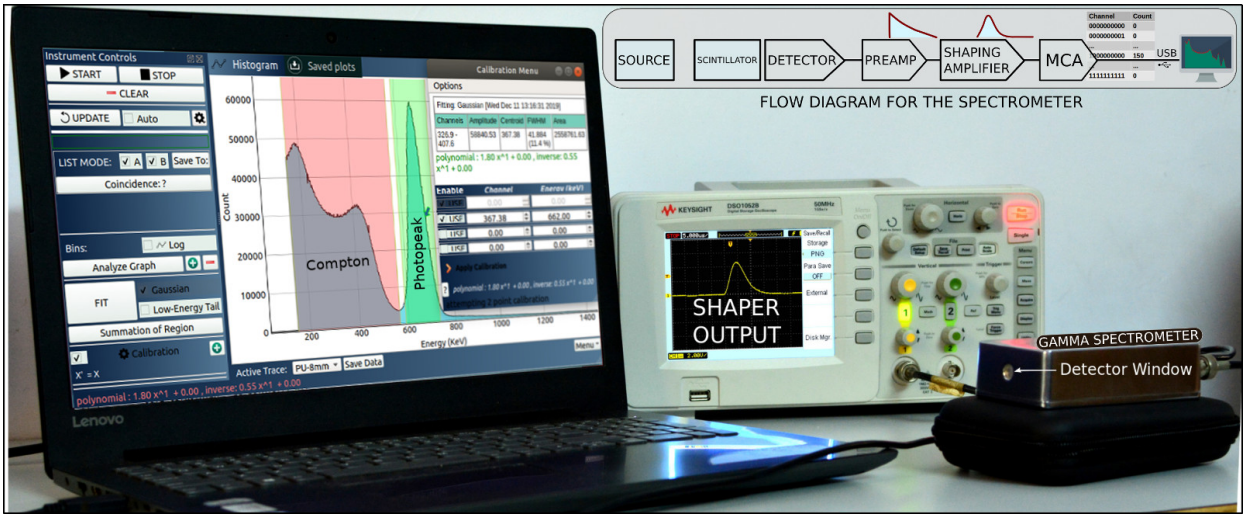

Figure 3: Photograph of the Gamma Spectrometer connected to a laptop showing the spectrum obtained. The shaper output is seen on the oscilloscope next to it, and the electronic circuit block diagram is shown as an inset.

fluctuations, in the absence of a signal. In order to reject this, the first 58 channels, that correspond to gamma energies upto 154keV, are not considered while acquiring spectra.

3.2 Data Acquisition

In the first iteration, the experiment is performed by simply placing approximately $20gm$ of Thorium Nitrate powder in front of a 2″ NaI scintillator attached to a PMT detector manufactured by Ortec. The data was acquired for a period of 2 hours, and the obtained spectrum is shown in Figure 4. Again, 20gm of Thorium Nitrate powder is placed in front of the GammaSpec-1K detector window. The data is acquired for a period of 3.5 hours with a 1K MCA, and the spectrum is shown in Figure 5. Since this spectrometer uses a 1K MCA, it will record higher counts per bin as compared to a 4K MCA with the same input range. This is because the 4K MCA has four times as many channels into which the total incident events can be distributed.

4 Analysis and Discussion

4.1 Determination of Energies in the Spectrum:

Due to the large number of gamma rays with distinct energies emitted by ^{232}Th and its daughters, multiple photopeaks are formed in the spectrum, with most of them being superimposed on the Compton scattered events of gammas with higher energies than them. The width of each photopeak is smeared across a few channels in the spectrum due to the limitations of the detector, and the centroid channel represents

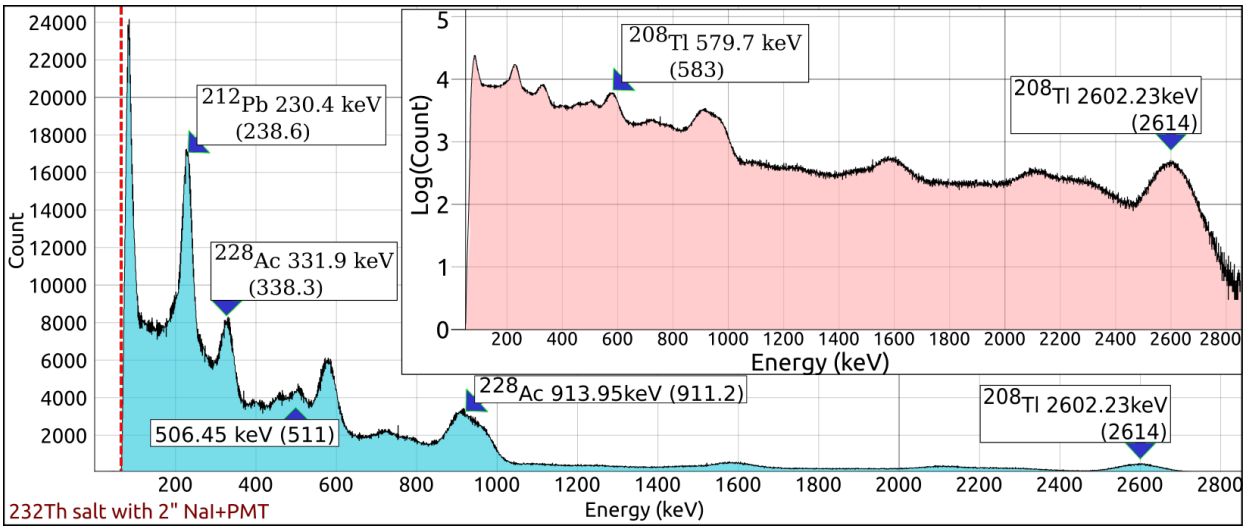

Figure 4: The Gamma spectrum of $ThNO_3$ powder obtained with a commercial PMT from Bicron with 2″ NaI scintillator and a 4K MCA.

Expected (in keV)	238.6	338.3	511	583	911	968.9	2614.5
2″ NaI(tl) + PMT	230.4	331.9	506.5	579.7	913.95	Unclear	2602.2
10mm CsI(Tl)+ Photodiode	235.6	339.0	508.5	580	913.6	966.6*	2607.2

Table 2: Comparison of peak centroids obtained from 20gm $ThNO_3$ sample from the two different detectors used. *Peak appears as a shoulder peak, and has been identified manually.

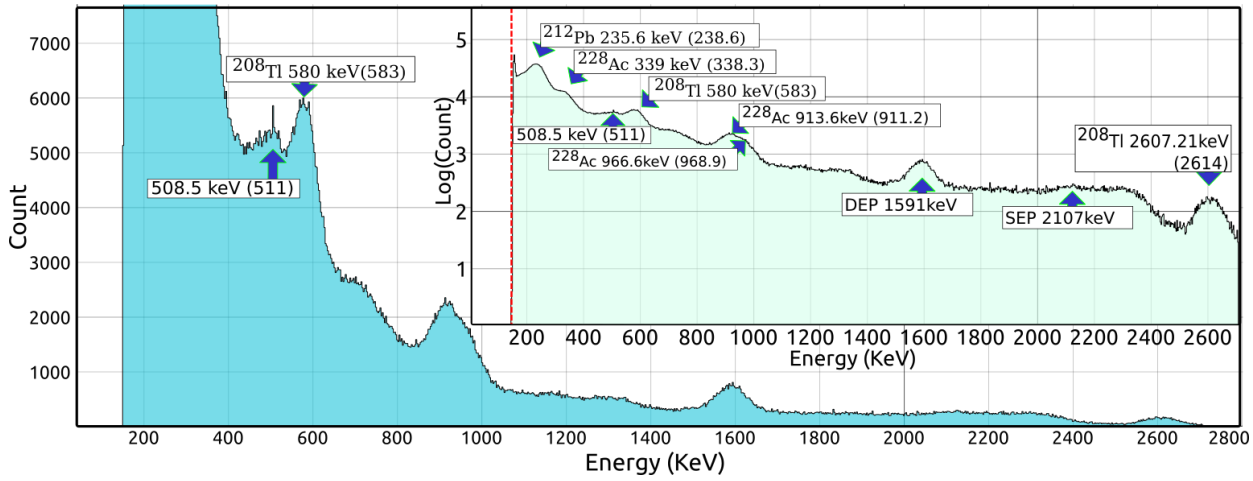

Figure 5: The Gamma spectrum of $ThNO_3$ powder obtained with GammaSpec1K spectrometer with CsI scintillator having volume $10mm * 10mm * 8mm$.

the actual peak position. Multiplying the centroid channel with the calibration polynomial gives us the energy associated with the peak. In order to extract the centroids which resemble a pseudo-gaussian shape, a mathematical least square minimization can be carried out on the channels containing the peak to identify the centroid. However, since this approach fails for small peaks riding on large Compton plateaus such as the 511 keV peak in Figure5, occasionally peak centers must be identified manually by estimating the channel spread of the photopeak. The energies obtained in both the spectra are tabulated in Table 2. We note that most of the energies expected from Table 1 are missing in the actual obtained spectrum. This is firstly due to the non-enriched source we are using, the energies due to transitions from I_α and I_β less than 5% do not emit enough gammas to be observed within the acquisition time. Further restrictions come due to the limitations of the detector units and the interaction processes within the detector medium which are discussed below:

4.1.1 Limitations of the detector unit

- All the energies less than 154 KeV shall be suppressed, corresponding to the 58 channel noise threshold we have set. That is, the gammas with energies that are not highlighted in the last column in Table 1 are to be ignored.

- The energies within the range of the FWHM, which is about 80-100KeV, cannot be resolved and shall appear at their weighted mean value. The resultant gammas to be expected, should form photopeaks in the spectrum at 238.6keV, 338.2, 481.9, 576.6, 940, and 2614.5 keVs.

4.1.2 Interations with the detector medium:

- Compton scattering produces a continuous range of energies below each of the expected energies.

- The gammas with energy greater than 1022 keV could result in pair production. In case of our $ThNO_3$ sample, the daughter product ^{208}Tl is responsible for the emission of gamma rays with 2614 keV energy which is capable of pair-production. The deposition of this energy resulting in pair production, and high chance of both annihilation photons escaping due to small detector volume, could result in a peak at 2612-1022=1590 keV, which is referred to as Double Escape Peak (DEP). Single escape event could result in 2614-511=2103 keV peak.

4.2 Efficiency Calculations for Comparision:

In order to make a comparison between the two detectors, we estimate the normalized efficiency. Even though the times of acquisition are not the same, the number of counts(N_E) for the low energy peak at 238

keV, medium energy peaks at 913 and 966 keV, and the largest energy peak at 2614.5 keV within the intervals that were chosen (see Table 3) about their photopeak width are determined. The total events N for the whole spectrum is also determined. The ratio $\frac{N_E}{N}$ indicates a normalized efficiency which can be used to compare the different detectors as long as the source is the same. However, since N_E includes Compton events from high energy peaks if any, the ratio may be overestimated and is only a reliable indicator for the highest energy peak, which in our case is 2614.5 keV. It is observed that the PMT based detector has an order of magnitude better normalized efficiency as compared to our spectrometer for this peak. The reduced overall efficiency of the smaller volume scintillator can be compensated by using longer acquisition time intervals. Since gamma interaction lengths are a function of energy, the smaller volume scintillator also shows a lower normalized efficiency ratio for the 2614keV gamma rays compared with the 238.6keV gamma rays.

5 Applications and Conclusions

5.1 Spectra of Monazite sample obtained using CsI Scintillator mated to PIN photodiode:

A 1gm Monazite sample procured from the sands of Kerala, and glued using Araldite epoxy on a 1" planchette was placed in front of the GammaSpec1K spectrometer, and the data acquired over a period of 14 hours is shown in Figure 6. All the expected peaks are identified and marked in the spectrum. It matches the one for $ThNO_3$ salt obtained in the lab, completely validating the utility of our spectrometer for environmental radiation monitoring.

5.2 Conclusions

We find that even though the volume of the scintillator used in our detector is around 130 times less than a standard 2" NaI scintillator, it is still usable for isotope identification. An added advantage is that high voltages are not required since our scintillator is mated with a photodiode instead of a PMT. The large volume scintillator however, has better photopeak efficiency, and lower Compton scattering, resulting in clearer peak formation. The capability to identify all the relevant peaks in Monazite sample makes our low cost, compact, portable USB powered Gamma Spectrometer an ideal choice for online radiation mapping of large geographical locations.

6 Acknowledgment

The authors thank Inter University Accelerator Centre(IUAC), New Delhi, for taking educational initiatives through their outreach programme, and providing a healthy environment for research and teaching in physics education. We would also like to thank Dr. K Sreekumar from Indian Rare Earths Ltd for introducing us to monazite sand and its expected characteristics.

Detector	Total Counts	Energy(keV)	Energy Interval(keV)	N_E	$\frac{N_E}{N}$
2″ NaI(Tl)		230.4	194.71-265.22	1079108	0.159
With	6768879	913.95+968.9	840-1030	5443016	0.08
PMT		2602.2	2516.83 - 2689.34	73771	0.01
10*10*8mm		235.6	201.26 - 270.11	856272	0.293
CsI(Tl) with	2914071	913.6+966.6	840 - 1030	122310	0.04
Photodiode		2607.2	2521.05-2693.18	2521.05	0.0024

Table 3: Determination of normalized efficiency for various energy peaks

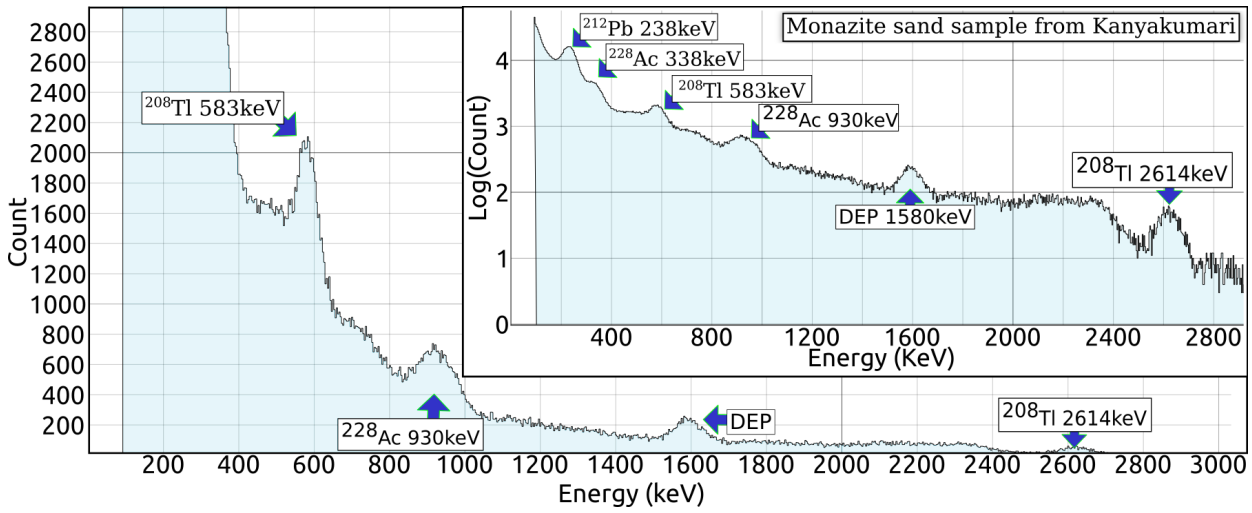

Figure 6: The Gamma spectrum of Monazite sample from the sands of Kerala. The peaks match those obtained from the Thorium Nitrate powder

References

[1] Swapna et.al 'Alpha Spectrum of 212-Bi Source Prepared using Electrolysis of Non-Enriched ThNO3 Salt', Physics Education-IAPT Volume 35: No. 1. Jan-Mar 2019.

[2] Jithin B.P., O.S.K.S Sastri. DAE Symp. on Nucl. Phys. 63 (2018) 1072 (pp. 10721073).

[3] Jithin et.al 'Measurement Model of an Alpha Spectrometer for Advanced Undergraduate Laboratories', Physics Education-IAPT Volume 35: No. 1. Jan-Mar 2019.

[4] Source code for CNspec `https://github.com/csparkresearch/cnspec/`

[5] `https://csparkresearch.in/alphaspectrometer/`

[6] Zwickl, Benjamin M., Noah Finkelstein, and Heather J. Lewandowski. "The process of transforming an advanced lab course: Goals, curricu-

lum, and assessments." American Journal of Physics 81, no. 1 (2013): 63-70.https://aapt.scitation.org/doi/10.1119/1.4768890

[7] Evaluated Nuclear Structure Data File Search and Retrieval, NNDC, Brookhaven National Laboratory. https://www.nndc.bnl.gov/ensdf/

[8] "Proposed syllabus and Scheme of Examination for B.Sc.(Honors) Physics" https://www.ugc.ac.in/pdfnews/7756304_B.SC.HONOURS-PHYSICS.pdf

[9] Martin, Brian R. Nuclear and particle physics: an introduction. John Wiley & Sons, 2006.

[10] Jithin B.P., O.S.K.S Sastri. DAE Symp. on Nucl. Phys. 64 (2019)

[11] https://csparkresearch.in/gammaspec/

[12] Sood, P. C. and Jain, Raj Kumar and Sastri, O. S. K. S., Unusual features of β transition rates in heavy deformed nuclei, Vol 69 Issue 5, May 2004, PhysRevC.69.057303, https://link.aps.org/doi/10.1103/PhysRevC.69.057303

[13] Gamma Detector white paper, First Sensor, DE. https://www.first-sensor.com/cms/upload/datasheets/gamma-ray-detection.pdf

[14] Tuli, Jagdish K. "NUCLEAR WALLET CARDS." (2011).

[15] CAEN N968 Spectroscopy Amplifierhttps://seltokphotonics.com/upload/iblock/dc3/dc32e13030d9a5c2fc1eb002e766554a.pdf

[16] CSpark Research Multi-Channel Analyzers https://csparkresearch.in/mca1k

[17] Franklin, A., The epistemology of experiment in Gooding, D. et al. (eds.) (1989) The uses of experiment: Studies in the natural sciences, Cambridge, UK: Cambridge University Press, 437-460.